Chapter 7
Review of On-Fault Palaeoseismic Studies Along the Dead Sea Fault

Shmuel Marco and Yann Klinger

Abstract The aim of this short note is to provide a summary over on-fault palaeoseismic works on the behavior of the Dead Sea fault (DSF). Key achievements of these studies include: the determination of slip rate of the DSF across different space and time resolutions, which converges at around 4–5 mm/a, confirmation of the sinistral relative motion between the Arabia Plate and the Sinai Subplate and of thrust motion and normal faulting associated with restraining bends and pull apart grabens respectively, and the verification of historical accounts on several strong earthquakes that were associated with surface ruptures. The comparison between the state-of-the-art slip-rate determinations along the DSF and the total motion accommodated by the known historical and instrumental earthquakes shows that current seismicity rates cannot account for the full slip rate. As previously proposed, the short-term rate of seismicity is not necessarily representative of the long-term seismic activity along the DSF. Assuming the historical records of the last two millennia are complete for strong earthquakes, we note long periods of quiescence in the sections of the northern Yammouneh, the Jordan Valley, and the southern Araba.

Keywords Dead Sea Transform fault • Tectonics • Active faulting • Earthquakes • Palaeoseismology • Middle East

S. Marco (✉)
Department of Geophysical, Atmospheric, and Planetary Sciences, Tel Aviv University, Ramat Aviv, Tel Aviv 69978, Israel
e-mail: shmulikm@tau.ac.il

Y. Klinger
Institut de Physique du Globe de Paris, Sorbonne Paris Cité, Univ. Paris Diderot, UMR 7154 CNRS, Paris, France
e-mail: klinger@ipgp.fr

Z. Garfunkel et al. (eds.), *Dead Sea Transform Fault System: Reviews*, Modern Approaches in Solid Earth Sciences 6, DOI 10.1007/978-94-017-8872-4_7,

7.1 Introduction

As early as 1869 Lartet suggested that Arabia and Africa have drifted apart to open up the Red Sea. Dubertret (1932) followed this idea suggesting a 160 km sinistral shear along the Dead Sea Fault associated with a 6° rotation between Arabia and Africa. Wellings (cited in Willis 1938) noted that this hypothesis corresponds to the offset of the marine Cambrian and Jurassic beds across the rift south of the Dead Sea. Willis (1938) rejected this hypothesis. During the following years, it was largely ignored until systematic research by Quennell (1956) provided evidence for 107 km sinistral slip. Later, with the advent of the plate tectonics, Freund and collaborators (Freund 1965; Freund et al. 1970, 1968) and Wilson (1965) recognized the Dead Sea rift as a transform fault zone that transfers the opening at the Red Sea to the collision zone at the Taurus-Zagros mountain belt.

The evidence for left-lateral shear along the Dead Sea Fault (DSF) since the early-middle Miocene is based on observations from four independent sources: regional plate tectonics, local geology, seismology, and geodesy. The plate tectonics shows that the opening of the Red Sea, where the Arabian plate is breaking away from Africa, is transferred to the collision with Eurasia via sinistral shear along the DSF (Freund 1965; Garfunkel 1981; Joffe and Garfunkel 1987; Quennell 1956). Sinistral motion explains the systematic offset of numerous pre-Miocene geologic features by a total of ~105 km, south of the Lebanon Restraining Bend (LRB) (Bartov et al. 1980; Freund 1965; Quennell 1956). Garfunkel et al. (1981) mapped the active fault traces of the DSF and associated these scarps with historical earthquakes that are reported from the region. Later research revealed prehistoric seismicity as well (Table 7.1 and Fig. 7.1). Focal mechanisms of moderate-to-large earthquakes show sinistral motion along the DSF (e.g. (Baer et al. 1999; Klinger et al. 1999; Salamon et al. 1996), Hofstetter et al. 2007). Geodetic measurements for the very short-term deformation are consistent with overall geologic observations of a sinistral slip-rate of 4–5 mm/year (Le Beon et al. 2008; McClusky et al. 2003; Reilinger et al. 2006; Wdowinski et al. 2004). In a review of the slip and seismicity of the DSF, Garfunkel (2011) concludes that the slip rate is slowing from an average rate of 6–7 mm/year over the last 5 Ma to 4–5.5 mm/year in the Pleistocene together with a slight eastward shift of the Euler pole of rotation between Sinai and Arabia.

Several authors noted explicitly that the detailed shape of the DSF had changed through time e.g. (Garfunkel 1981; Heimann and Ron 1987, 1993; Rotstein et al. 1992; ten Brink et al. 1999; ten-Brink and Ben-Avraham 1989). For the section south of the LRB, the widest zone of distributed faulting is about 50 km wide. It is found in the Galilee, where the early-stage (Miocene) faults were associated with formation of basins (Freund et al. 1970; Shaliv 1991) and with rotation of rigid blocks about sub-vertical axes (Ron et al. 1984), although the linkage to the transform movement is not well established. In this region, subsequent post-Miocene deformation took place mostly in the form of normal faulting on E-W trending faults with some strike-slip motion currently localized in a very narrow zone.

Table 7.1 List of on-fault palaeoseismic investigations at the DSF system arranged by time of publication

# in Fig. 7.1	References	Segment	Observations	Fault type	Achievement Earthquakes/ Slip Rate (SR)/Last Event (LE)/Recurrence (Re)
1	Reches and Hoexter (1981)	S. Jordan Valley	Trenches	N	31 BCE, 747 CE
2	Marco and Agnon (1995)	Dead Sea	Outcrops	N	Re
3	Amit et al (1996, 1999, 2002)	Southern Arava	Trenches	N	Re
4	Marco et al.; Ellenblum et al. (1998)	Jordan Gorge	Trenches, archaeology	LL	1202, 1759
5	Galli (1999)	Arava-Jordan-Hula Valley	Outcrops, archaeology	LL	
6	Enzel et al. (2000)	Dead Sea	Outcrops	N	Re
7	Klinger et al. (2000a)	Northern Arava	Archaeology, outcrops	LL	1212
8	Klinger et al. (2000b)	Northern Arava	Outcrops	LL	SR
9	Niemi et al. (2001)	Northern Arava	Outcrops	LL	SR
10	Zilberman et al. (2000)	Hula Valley	Trenches	N	
11	Gomez et al. (2001, 2003)	Serghaya Fault	Trenches, Outcrops	LL	1705 or 1759/
12	Meghraoui et al. (2003)	Misyaf, Yammouneh	Trenches, archaeology	LL	
13	Marco et al. (2003)	Sea of Galilee	Archaeology	N	749
14	Daëron et al. (2004, 2005, 2007)	South Yammouneh	Trenches	LL	1202
15	Zilberman et al. (2005)	South Arava	Trenches	N	3/1068/
16	Marco et al. (2005)	Jordan Gorge	Trenches	LL	1202, 1759/LE/SR
17	Chorowicz et al. (2005)	Yammouneh	Outcrops	LL	SR
18	Akyuz et al. (2006)	Northern Yammouneh	Trenches, Outcrops	LL	859, 1408, 1872
19	Nemer and Meghraoui (2006)	Roum Fault	Trenches, Outcrops	LL	1837, SR
20	Haynes et al. (2006)	Northern Arava	Archaeology	LL	634 or 659/660, 873, 1068, and 1546
21	Elias et al. (2007)	Lebanon thrust	Outcrops	R	551 CE/
22	Thomas et al. (2007)	Aqaba	Archaeology	LL	
23	Ferry et al. (2007)	Jordan Valley	Outcrops	LL	SR
24	Le Beon et al. (2008)	Arava	Outcrops	LL	

(continued)

Table 7.1 (continued)

# in Fig. 7.1	References	Segment	Observations	Fault type	Achievement Earthquakes/ Slip Rate (SR)/Last Event (LE)/Recurrence (Re)
25	Nemer et al. (2008)	Rachaya and Serghaya faults	Outcrops, trenches	LL	1759
26	Makovsky et al. (2008)	Elat Fault	Submarine geophysics	LL	SR
27	Altunel et al. (2009)	S. Turkey	Trenches, archaeology	LL	SR
28	Le Beon et al. (2010)	Arava	Outcrops	LL	SR
29	Karabacak et al. (2010)	Northern Yammouneh	Outcrops	LL	SR
30	Ferry et al. (2011)	Jordan Valley	Trenches, archaeology	LL	SR, Re, LE
31	Le Beon et al. (2012)	Arava	Outcrop	LL	SR

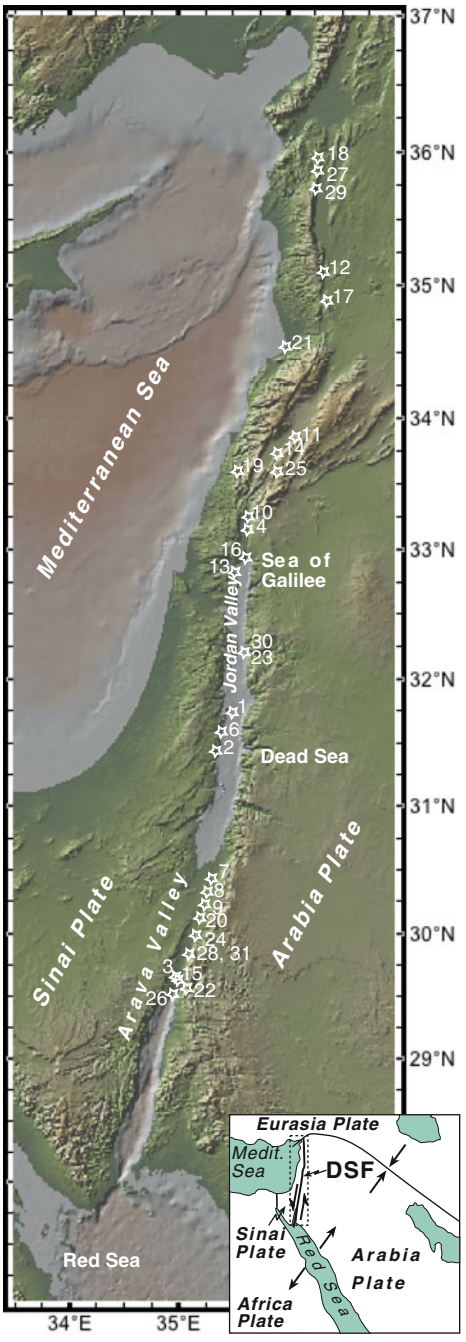

Fig. 7.1 Location of palaeoseismic studies along the Dead Sea Fault. Numbers refer to entries in Table 7.1

The deformation further south is characterized by a 20–30-km-wide zone with primarily strike-slip and some normal slip on faults trending sub-parallel to the main transform fault. The location of the active fault strands along the Dead Sea Transform fault zone (DSF) changed through time. In the western margins of Dead Sea basin, the early activity began a few kilometers west of the present shores and moved toward the center of the basin in four stages. Similar basinward migration of faulting is apparent in the Hula Valley north of the Sea of Galilee as well as in the Negev and the Sinai Peninsula. In the Arava Valley, seismic surveys reveal a series of buried inactive basins whereas the current active strand is located along the eastern margin. In general, the faulting along the DSF became localized by the end of the Miocene. The subsidence of fault-controlled basins in the early stage, stopped at the end of the Miocene. During the Plio-Pleistocene, new faults were formed in the Negev west of the main transform, possibly manifesting another cycle that has begun with the widening of the fault zone (Marco 2007).

This paper reviews the contribution of recent studies on the most recent activity of the DSF (mostly its southern section, south of the LRB) and its subsidiary faults. These studies contributed to the recognition of the active strands in the fault zone, constrained the slip rates and recurrence intervals of the various fault segments, and determined the time of the last slip event after which the segment had remained locked. The offset geological and archaeological bodies confirm the plate tectonics paradigm and provide an independent examination of the structural complexities such as restraining bends, pull-apart basins, and distributed slip among fault branches. The fault was characterized as a "leaky transform" because of these pull-aparts (Garfunkel 1981). The temporal overlap of geological and historical-archaeological information provides important crosschecks of the sources of data. On-fault research requires the identification of faults. This is relatively easy where the fault zone is narrow and exposures are good. It is less complete where the fault zone is wide and consists of many branches, or where the faulting activity shifts location and young sediments or basalt flows cover the faults.

7.1.1 Detailed Mapping of the Fault Zone

The first detailed maps of the DSF zone that emphasized the offset of Pleistocene to sub-recent units were published by Garfunkel et al. (1981). Various structures such as pull apart grabens, restraining bends, branching faults, and folds, which comprise the fault zone were also described and analyzed at the same time (Eyal et al. 1981; Garfunkel 1981). The recognition of small displacements of young geological features such as alluvial fans or lake deposits opened the road for neotectonics and palaeoseismic research. These studies showed that the fault consists of numerous segments separated by discontinuities or sharp changes in their strike. A GIS-based map of the faults suspected as being "active" (Bartov et al. 2002) was generated by defining active faults as those that either cross or bound Pliocene and younger

stratigraphic units. It is not clear yet whether the strong earthquake ruptures are arrested at the mapped segment ends. This question is important because the length of the ruptures correlates with the earthquake size (e.g., Wells and Coppersmith 1994). The detailed maps reveal that the structure of the DSF is variable (described from south to north): The southernmost part is the Gulf of Aqaba-Elat, where a series of left-stepping, en-echelon fault arrangement forms three elongate deep pull-apart basins separated by shallow thresholds (Ben-Avraham and Garfunkel 1979). The largest earthquake (M7.2) ever recorded instrumentally occurred in the gulf on November 22, 1995 (Klinger et al. 1999; Pinar and Turkelli 1997; Shamir et al. 2003). The next section toward the north is the Araba Valley, characterized by a narrow fault zone that offsets a series of Pleistocene-Holocene alluvial fans (Garfunkel et al. 1981). Several palaeoseismic studies quantify the displacements (Klinger et al. 2000a; Le Beon et al. 2010, 2012; Niemi et al. 2001). Seismic reflections reveal that the subsurface structure of the Araba Valley includes buried Miocene grabens (Frieslander 2000). The next section is the pull-apart basin of the Dead Sea, where two sub-parallel faults bound the deepest place on the Earth continents. The Dead Sea pull-apart structure is bounded by the Amaziahu Fault on the south, where a sharp scarp in Late Pleistocene lake deposits reaches a height of up to 30 m. The northern boundary does not have a surface expression. The western fault continues due north along the Jordan Valley, where it is recognized as a narrow fault zone in Pleistocene sediments (Ferry and Meghraoui 2008; Ferry et al. 2007; Garfunkel et al. 1981). Two faults branch off the main fault zone. One at the northeastern end of the Dead Sea a NE-striking fault scarp manifests normal slip component, and the second, further north, a NW-striking fault branches off the Bet She'an Valley, also has a normal slip component with Mount Gilboa at the footwall. The northern end of the Jordan Valley section is where the fault zone consists of two parallel faults, which form the graben structure of Kinarot and the Sea of Galilee further north. The western boundary fault of the southern Sea of Galilee bends westward, making the northern part of the basin wider. This branch crosses the town of Tiberias (Hazan et al. 2004; Marco et al. 2003). The eastern boundary fault bends northeastward. In contrast to the dual fault at the south there is a single fault to the north of the Sea of Galilee, known as the Jordan Gorge Fault, which offsets manmade structures (Ellenblum et al. 1998) and Holocene stream channels (Marco et al. 2005; Wechsler et al. 2011). The Hula pull-apart basin to the north of the Jordan Gorge section is also where the fault system splays into several branches, namely (east to west) the Rachaia Fault, Serghaia Fault, Yammouneh Fault, and Roum Fault (Fig. 2). The Yammouneh, which takes up most of the plate motions, continues northward to the triple junction in southern Turkey, where it joins the East Anatolian Fault on the northeast and the Eastern Mediterranean collision zone on the west.

The on-fault studies resolve the debate revolving around the identification of the active branch. The suggestions that the main active fault is the Carmel Fault (Girdler 1990) or the Roum Fault (Butler et al. 1997, 1999) are not supported by the observations. Although they do take a small portion of the plate motions, the Yammouneh exhibits the major activity as well as the most prominent topographic feature,

with some local contribution of the Lebanon Bend-related Rachaya-Serghaia fault branches (Daëron et al. 2005, 2007; Fleury et al. 1999; Gomez et al. 2003). Palaeoseismic records from the DSF in Syria and in southern Turkey also reveal major earthquake ruptures along the northern extension of the DSF (Akyuz et al. 2006; Altunel et al. 2009; Karabacak et al. 2010; Meghraoui et al. 2003). The analysis of three GPS campaigns between 1996 and 2008 shows an oblique motion along the Carmel Fault with about 0.7 mm/year left-lateral and about 0.6 mm/year N-S extension (Sadeh et al. 2012).

7.1.2 Test Plate Tectonic Paradigm

The debates on the nature of movement along the DSF (e.g., Vroman 1973) have been replaced by widely-agreed consensus on its left-lateral sense. Euler's theorem provides the means for resolving the relative motion on any one of three plate boundaries in a triple junction given the motions of the other two. The DSF connects the northern Red Sea spreading center to the collision zone located in South Eastern Turkey. If the fault were a pure transform, i.e., along a perfect small circle, the calculated DSF motion should be the same when solved for either junction, and this should conform to results from the DSF itself. In practice, the determination of accurate slip rates at both the southern end of the DSF, where it connects with the Red Sea and the Gulf of Suez, and at the northern end, where it connects with the East Anatolian fault and the subduction zone of the Cyprus arc, are poorly constrained and do not allow for such theoretical proof. Qualitative and quantitative confirmation for sinistral movement along the DSF, however, are validated by numerous observation of sinistral displacements of geological and archaeological bodies, as well as normal displacements of strata at the margins of pull-apart basins and all along the DSF itself. At present, the slip rates determined by the palaeoseismic studies alone (Table 7.3) are too variable to provide a definite quantitative confirmation of the plate tectonic models. Many of the on-fault palaeoseismic studies document the vertical components of slip. The few locations with suitable markers for measuring strike slip invariably confirm the sinistral nature of the motion. These data include offset alluvial fans (Garfunkel et al. 1981; Klinger et al. 2000a; Le Beon et al. 2010, 2012; Niemi et al. 2001), stream channels (Ferry et al. 2007; Marco et al. 2005; Wechsler et al. 2011), and archaeological structures (Table 7.1).

7.1.3 Earthquake Activity – History, Prehistory

Instrumental seismology along the DSF is limited to only one strong earthquake, the M_W7.2, 1995 Nuweiba, and one moderate, M_L6.1, 1927 Jericho earthquake. In order to recover earthquake history we must combine historical records, archaeological observations, and geological evidence for earthquake fault ruptures. All three kinds

of data can either relate to off-fault or on-fault phenomena. The off-fault effects are reviewed by A. Agnon in Chapter 8. The on-fault research essentially relies on identification of surface, or near-surface, disruptions of geomorphic features, soil layers and man-made structures, either naturally outcropping or exposed in man-made trenches.

The first palaoeseismic trench was opened near Jericho across the fault trace identified by Garfunkel et al. (1981). Offset strata were dated using indicative archaeological artifacts (Reches and Hoexter 1981) and interpreted as the ruptures of the historically-recorded earthquakes of 31 BCE and 747 CE. Another set of pioneering palaeoseismic research trenches explored slip on normal faults and the development desert soils as a means to decipher tectonics at the western border of the fault zone in the southern Arava (Amit et al. 1995; Gerson et al. 1993). Several studies were aided with geophysical detection of faults, e.g., by GPR (Basson et al. 2002), high-resolution seismic reflection (Marco et al. 2005; Agnon et al. 2006), and magnetic field (Altunel et al. 2009). These, and later on-fault palaeoseismic observations, are summarized in Table 7.1.

7.2 Achievements of DST On-fault Studies

7.2.1 Test Reliability of Historical Records

Abundant accounts on historical earthquakes have been catalogued (e.g., Ambraseys 2009; Ambraseys and Finkel 1995; Ambraseys et al. 1994; Amiran et al. 1994; Guidoboni and Comastri 2005; Guidoboni et al. 1994; Russell 1985; Sbeinati et al. 2005). The catalogues include descriptions of damage to property, natural phenomena, human reactions, and fatalities. Reference to fault ruptures are usually missing. It is assumed that this lack of reference is not because there were no surface ruptures but rather because the contemporary reporters of these accounts were not aware of the association between earthquakes and faulting. Hence, pairing an historical earthquake to a specific fault often remains difficult. A major uncertainty is related to dating because the commonly used methods in palaeoseismic research, namely radiocarbon and luminescence, have large error margins and these need to be correlated with the often-uncertain dates of reported earthquakes. Several authors have pointed out the pitfalls of potential circular reasoning (e.g., Ambraseys 2005; Marco 2008; Rucker and Niemi 2010). Commonly, the geologists who find evidences for past earthquakes look for records of historical earthquakes listed in catalogues whose dates fall within the geological dating ranges. This practice works fine for the section south of the Hula Valley, where the fault zone is relatively simple. It is less certain for the fault zone farther north, where several branches, in addition to the Yammouneh fault that continues northward to Turkey, may be associated with strong earthquakes.

Table 7.2 Historical DSF earthquakes confirmed by surface ruptures observed in palaeoseismic investigations

Locations Fig. 7.1	Date	Segment	References
1	31 BCE	Jordan Valley	Reches and Hoexter (1981)
12	115 CE	Misyaf, Yammouneh	Meghraoui et al. (2003)
21	551	Lebanon thrust	Elias et al. (2007)
13, 1	749	Jordan Valley	Marco et al. (2003) and Reches and Hoexter (1981)
18	859	Northern Yammouneh	Akyuz et al. (2006)
15	3/1068	South Arava	Zilberman et al. (2005)
12	1170	Missyaf, Yammouneh	Meghraoui et al. (2003)
14, 4	1202	South Yammouneh	Daëron et al. (2005), Ellenblum et al. (1998), and Marco et al. (1997, 2005)
8, 9	1212	Northern Arava	Klinger et al. (2000b) and Niemi et al. (2001)
18	1408	Northern Yammouneh	Akyuz et al. (2006)
8	1458	Northern Arava	Klinger et al. (2000b)
11	1705	Serghaya Fault	Gomez et al. (2001)
4, 16	10/1759	Jordan Gorge	Ellenblum et al. (1998), Marco et al. (1997), and Marco et al. (2005)
14, 11, 25	11/1759	Serghaya Fault	Daëron et al. (2005), Gomez et al. (2001), and Nemer et al. (2008)
19	1837	Roum Fault	Nemer and Meghraoui (2006)
18	1872	Northern Yammouneh	Akyuz et al. (2006)

An example of successful matching between geological and archeological data is found at the site of Ateret, where structures were built on top of the active fault. There, accurate measurements of the slip associated with the earthquakes of 1202 and 1759 CE were possible (Ellenblum et al. 1998; Marco et al. 1997). Palaeoseismic trenches dug some 10 km southward confirmed these archaeoseismic results (Marco et al. 2005; Wechsler et al. 2011), while trenches along the Yammouneh fault (Daëron et al. 2005, 2007) were crucial to determine the northward extension of the ground ruptures associated with these two events. The rupture sizes and locations are remarkably in accord with independent analysis of historical reports on these earthquakes (Ambraseys and Barazangi 1989; Ambraseys and Melville 1988; Sieberg 1932). Table 7.2 lists all the historical records that were confirmed by direct observations. The observations include faulted strata and archaeological structures. The evidence for surface ruptures indicates that the earthquakes magnitudes were greater than M6, and that the historical records are largely reliable in such magnitude range.

Assuming the historical earthquake catalogues of earthquakes that were not confirmed yet by geological studies are also reasonably reliable, we illustrate their locations along the DSF system (Fig. 7.2). We interpret the locations to be close to the maximum reported damage area, although ideally it would be better if more data were available and more robust objective methods could be used (e.g., Bakun and Wentworth 1998; Sirovich et al. 2002; Zohar and Marco 2012).

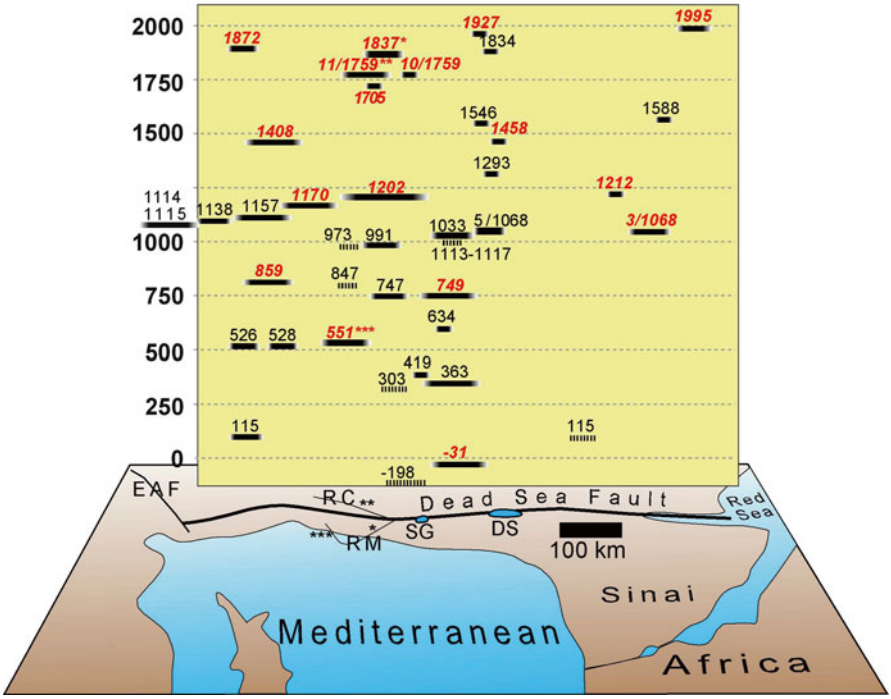

Fig. 7.2 Historical earthquakes distribution in space and time. Each bar corresponds to an approximate earthquake location along the DSF at the map. *Red dates* are earthquakes whose ruptures were found in palaeoseismic studies (see Table 7.2). Abbreviations: *EAF* East Anatolia Fault, *RC* Rachaya Fault, *RM* Roum Fault, *SG* Sea of Galilee, *DS* Dead Sea (Partly based on Garfunkel et al. 1981)

7.2.2 Slip Rate – Miocene to Holocene

Dated geological slip markers of two kinds are used for constraining slip rate (Table 7.3). One kind is pre-Miocene, which determines the total offset and thus the long-term slip rate. The other kind uses features that formed while the DSF was active, which determine short-term rates of individual sections of the fault. Palaeoseismic studies aim in particular at the Pleistocene-Recent activity. The short-term slip rate may be used for estimating the slip deficit by assuming that the total slip is represented either by the long-term slip rate, and/or the geodetically measured velocity away from the plate boundary. Along the southern section of the DSF, a minimum long-term rate is determined by dividing the 107-km total slip that is determined from the offset of pre-DSF geologic features visible both in the Negev and in Jordan, by the time of earliest faulting, about 20–25 Ma ago. The youngest rock unit that is offset by the full 107 km are 20-Ma dikes exposed in Sinai and Arabia (Bartov et al. 1980), providing a minimum long slip rate of about 5.35 mm/year. The motion post-dates the dikes but the precise initiation time is unclear yet.

Table 7.3 Slip rate estimates of the DSF

Period	Span, Ma	Rate mm a^{-1}	Max	Min	Data	Published	Reference
	?				Geological	1947	Dubertret (1947)
Miocene	?	5			Geological	1956	Quennell (1956)
Late Pleistocene-Recent	0.1	10			Geological	1968	Freund et al. (1968)
7–10 Ma	10	5 ± 1	4	6	Geological	1970	Freund et al. (1970)
Last 1,000 years	0.001	0.8–1.7			Historical seismicity, magnitudes estimates based on extent of damage, seismic moment based on M-Mo empirical relation in California	1981	Garfunkel et al. (1981)
Plio-Pleistocene	5	7–10			Geological	1981	Garfunkel et al. (1981)
Last 4,500 years	0.0045	2.2			Estimates of slip associated with historical seismicity. Based on the assumption of GR relation extrapolated to high M earthquakes	1981	Ben-Menahem (1981)
20 Ma	20	5.1 ± 0.3	4.8	5.5	Total offset, initiation based on pre-DSF dikes. Minimum rate. Dating – composite isochron	1981	Eyal et al. (1981)
1733 years section in the Late Pleistocene	0.0017	6.4 ± 0.4	6	6.8	Recurrence based on deformed uppermost Lisan beds, rate of seismicity, assuming GR $\log N = 5.24–0.68\,M$ calculated from the 1733-year-long section	1986	El-Isa and Mustafa (1986)
Plio-Pleistocene	5	20			Geological, based on offset travertines in northern Hula Valley	1986	Steinitz and Bartov (1986)
Plio-Pleistocene	5	6 (0.283°/Ma)			Plate kinematics	1987	Joffe and Garfunkel (1987)
Holocene	0.01	>0.7			Geological, secondary deformation	1990	Gardosh et al. (1990)
Plio-Pleistocene	5	5.4–6.1			Geological	1990	Heimann (1990)
Plio-Pleistocene	5	3–7.5			Drainage systems, Arava Fault	1998	Ginat et al. (1998)

Late Pleistocene-Holocene	0.1	≥10			Offset fans	1999	Galli (1999)
Pleistocene	2	2–6, prefer 4			Alluvial fans, N. Arava	2000	Klinger et al. (2000a)
Pleistocene	2	4.7 ± 1.3			Alluvial fans, Arava	2001	Niemi et al. (2001)
Holocene	0.01	1–2			Serghaya Fault	2001	Gomez et al. (2001)
Last 2,000 years	0.002	6.9 ± 0.1			Displaced aqueduct; Paleo and Archaeoseismology, Missyaf (DSF in Syria). Assuming straight original shape	2003	Meghraoui et al. (2003)
1996–1999	0	2.6 ± 1			Geodesy, GPS	2003	Pe'eri et al. (2002)
Survey-Mode GPS	0	5.6–7.5			Increase from south to north	2003	McClusky et al. (2003)
Holocene	0.01	1.4 ± 0.2			Serghaya Fault	2003	Gomez et al. (2003)
1996–2003	0	3.3 ± 0.4			Geodesy, GPS results mostly on W side of fault. Based on model assuming fit to arctangent and locking depth	2004	Wdowinski et al. (2004)
25 ka	0.025	3.8–6.4	3.8	6.4	Geological, Lebanon	2004	Daëron et al. (2004)
Last 5,000 years	0.005	≥3	3	–	Single stream channel, Jordan Gorge. Northern margin offset 15 m, southern margin 9 m. C14 age of bulk organic matter. Minimum for that point, fault zone may be wider than trench	2005	Marco et al. (2005)
Last 6 Ma	6	c. 3.3			Offset c. 6 Ma NW margin of the Shin Volcano by c. 20 km	2005	Chorowicz et al. (2005)
1996–2003	0	4.4 ± 0.3			GPS	2005	Mahmoud et al. (2005)
Last 47.5 k years	0.0475	4.7–5.1 mm/year			Offset channels incised into the Lisan, Jordan Valley. Main channel predates highest stand	2007	Ferry et al. (2007) Comment/Reply: Ferry and Meghraoui (2008) and Klein (2008)
4 years	0		4	5	GPS	2007	Gomez et al. (2007)

(continued)

Table 7.3 (continued)

Period	Span, Ma	Rate mm a^{-1}	Max	Min	Data	Published	Reference
1999–2005	0	4.9 ± 1.4			GPS	2008	Le Beon et al. (2008)
Holocene	0.01	2.7 ± 1.5			Offset reef	2008	Ma kovsky et al. (2008)
Last 2,000	0.002	>2.8 ± 0.2			Offset Hellenistic walls, Ateret,	–	Agnon et al. (2010)
7 kyears	0.007	6			Offset archaeology	2009	Altunel et al. (2009)
8 years	0	1.8–3.3			GPS	2010	Alchalbi et al. (2010)
25 ka	0.025	5			Offset channels, archaeology	2011	Ferry et al. (2011)
141 ka	0.141	5.4 ± 2.7			Offset channels	2011	Le Beon et al. (2010)
		4.5 ± 0.9					
		8.1 ± 2.9					
Last 300 ka	300 ka	5–7			Offset channels	2012	Le Beon et al. (2012)

The consistency of instantaneous GPS rates (Le Beon et al. 2008), Quaternary rates (Klinger et al. 2000a; Niemi et al. 2001; Le Beon et al. 2010, 2012) and several-millions-years-long slip rates (Bartov et al. 1980) stands out. However it contrasts with the large variability of rates determined by paleoseismological studies and archaeological markers. For example, offset of a Roman period aqueduct is interpreted to show 7 mm/a (Meghraoui et al. 2003) whereas offset walls from the late twelfth century are offset only 2.1 m (Ellenblum et al. 1998). This may be explained either by distributed deformation unaccounted for by on-fault palaeoseismic investigations or, more probably, by too short time-windows of observation along some fault segments spans.

The discrepancy between short-term slip rates calculated by adding earthquake ruptures, and long-term rates is referred to as slip deficit. The long-term rate of 105 km slip in 20–25 Ma is 4–5 mm/year, in agreement with GPS results. Garfunkel et al. (1981) assigning sinistral slip to most of the historical earthquakes along the DSF, estimated that the sum of the seismic slip accounts for about two thirds of the long-term slip. Salamon et al. (1996) focusing only on the twentieth century seismicity found that only 7 % of the long-term slip was accommodated by earthquakes, leaving 83 % of the slip needed to match the long term slip-rate unexplained. Hence, such calculations show with little ambiguity that one needs to be able to document earthquake time series significantly longer than one earthquake cycle to be able to know something sensible about slip-rates from paleoseismology (Wechsler et al. 2011). This is particularly evident where the seismic activity might not be homogeneous but rather clustered, as it has been suggested for the DSF (Marco et al. 1996). And yet, the results of the palaeoseismic studies on the main strand of the DSF, which span enough time, are also in agreement with the geodetic and with the long-term rates (Ferry et al. 2011; Klinger et al. 2000a; Le Beon et al. 2010; Niemi et al. 2001).

7.2.3 Structural Details, Pull-Aparts, Thrusts

Structurally complex sections along the DSF include overlapping segments, commonly associated with pull-apart basins, right jogs where push-up swells occur, and splay faults of various strike directions. These complexities give rise to a variety of types of faults.

Thrust faults are mostly common along the Lebanese Restraining Bend (Elias et al. 2007) and the nearby Palmyride folds range, in Syria (Abou Romieh et al. 2012; Alchalbi et al. 2010; Chaimov and Barazangi 1990). Also the slip rates on the different thrust faults outcropping in these two areas is still subject to active discussion, the thrust associated to the LRB seems to be currently the most active with several large historical earthquakes associated with these structures.

Normal faults are usually associated with the occurrence of pull-apart basins (Garfunkel 1981), although several normal faults are also visible in the region of Galilee. Morphological analyses and palaeoseismic trench studies at the margins of the southern Arava confirm the normal nature of the fault on the west (Amit et al. 2002, 1999; Zilberman et al. 2005) and on the east (Thomas et al. 2007). Holocene activity of normal faults has been documented at the eastern boundary fault of the

Hula pull-apart valley (Zilberman et al. 2000). In Tiberias city, on the western shore of the Sea of Galilee, a normal fault offset early eighth century CE buildings, whereas late eighth century buildings located on top of the fault are not affected, bracketing an earthquake during the eighth century (Marco et al. 2003). Late Pleistocene normal fault zones were documented as active during the deposition of the Lisan Formation, at the western margins of the Dead Sea Basin (Bartov and Sagy 2004; Marco and Agnon 1995, 2005). On the western bounding fault of the Gulf of Aqaba Shaked et al. (2004, 2012) reconstruct vertical movements by dating buried coral reefs and submerged archaeological site. These palaeoseismic studies confirm the "leaky" nature of the DSF (Garfunkel 1981) and the paradigm of pull-apart structures (rhomb grabens) along strike-slip faults.

The structural role and history of activity of apparently "incongruent" faults that strike NE but show normal displacement instead of reverse motion that is expected to conform with NW-SE shortening, are not explored yet. These include the Sheikh Ali Fault at the NE end of the Sea of Galilee, a fault at the NE corner of the Dead Sea, and the NE corner of the Gulf of Aqaba. The NW-SE extension there is incompatible with the maximum horizontal compression that is inferred on the basis of analysis of meso-structures in the region (Eyal and Reches 1983).

7.3 Discussion

On-fault studies have confirmed the location of the main active strands of the DSF. In many cases, those studies have also brought new information about past earthquakes, documented, or not, in historical records. Building on these observations, we try to interpret the space-time distribution of earthquakes over the last two millennia (Fig. 7.2) and to suggest that a short-term pattern, periods without significant seismicity alternating with periods of intense activity, might exist.

Several earthquakes appear to define a seismic sequence rupturing from north to south. The most conspicuous series starts with the 1114/1115 CE earthquakes on the East Anatolian Fault and continues with the earthquakes of 1157, 1170, and 1202 CE. If these sequences indeed happen as outlined above, we do not see a similar or repeat pattern in the past. If this is correct, the famous North Anatolian Fault sequence of the 20th century, when a sequence of strong earthquake ruptures began on the east and propagated westward (Barka 1996; Stein et al. 1997) may not be a recurring sequence either.

Striking quiescence periods, of the order of several hundreds of years, appear to indicate imminent ruptures of several section of the fault. The segment between the Sea of Galilee and the Dead Sea ruptured in 31 BCE, 363 CE, 749 AD, and 1033 CE, followed by a millennium-long quiescence in which only moderate earthquakes occurred. The northern segment in Syria has been quiet for over 8 centuries (Meghraoui et al. 2003). Finally, the southern segment of the DSF along the Wadi Araba, has apparently not ruptured significantly for at least six hundred years. One might wonder if the Mw7.3 Nuweiba earthquake in 1995 in the Gulf of Aqaba marks the beginning of a new seismic sequence that could rupture a longer section of the DSF in the near future.

The estimated Late Pleistocene – Holocene slip rates seem to converge between 4 and 5 mm/year. The long-term rates that are based on offset Miocene and Pliocene geological bodies are in agreement with plate motion rates as determined geodetically. We therefore regard the variation in palaeoseismically-determined rates as indications of insufficient temporal coverage for some segments. The conversion of modern seismicity to slip also does not amount neither to the long-term slip nor to the geodetic slip rate (Garfunkel 2011), most probably because it represents a short time.

7.3.1 Future Targets

More data are needed to examine whether ruptures stop at mapped segment boundaries. We can at least confirm that several large earthquakes, such as the 1202 rupture, went through segment boundaries. Smaller earthquakes such as the October 30, 1759 were probably confined to a single segment but there are no data from the adjacent segments that could definitely rule out ruptures there as slip partitioning occurs where parallel or sub-parallel fault segments occur, e.g., the bounding faults of pull-apart grabens and where there are branches that split off the main fault, e.g., the Carmel Fault, Serghaya Fault, and Roum Fault.

The rupture history of transverse faults that connect overlapping faults at the boundaries of pull-apart basins is also unknown. To date none of the palaeoseismic studies addressed faults such as the Amatzyahu Fault that forms the southern boundary of the Dead Sea. These faults may either act independently or as rupture terminations of longer strike-slip faults. Comparisons of palaeoseismic records can reveal which is correct.

The structural role of the extension features at the NE corners of the Gulf of Aqaba, the Dead Sea, and the Sea of Galilee is unclear yet. Exploring the NE-SW-striking normal faults that appear in all these locations and express "incongruent" ~ NW-SE extension can shed light on these structures.

Acknowledgments Partial funding was provided by the Israel Science Foundation grant 1736/11 to SM.

References

Abou Romieh M, Westaway R, Daoud M, Bridgland DR (2012) First indications of high slip rates on active reverse faults NW of Damascus, Syria, from observations of deformed Quaternary sediments: implications for the partitioning of crustal deformation in the Middle Eastern region. Tectonophysics 538–540:86–104

Agnon A, Migowski C, Marco S (2006) Intraclast breccia layers in laminated sequences: recorders of paleo-earthquakes. In: Enzel Y, Agnon A, Stein M (eds) New Frontiers in Dead Sea paleoenvironmental research. Geological Society of America Special Publication, Boulder, pp 195–214

Agnon A, Marco S, Sagy A, Ellenblum R (2010) Discrepancy between GPS (5 yrs) and archaeoseismic (3 kyr) slip rate across the Ateret site (Dead Sea fault): secular variations versus

distributed slip. In: Proceedings AGU Fall meeting abstracts, San Francisco, CA, vol 1. American Geophysical Union, p 2206

Akyuz HS, Altunel E, Karabacak V, Yalciner CC (2006) Historical earthquake activity of the northern part of the Dead Sea Fault Zone, southern Turkey. Tectonophysics 426:281–293

Alchalbi A, Daoud M, Gomez F, McClusky S, Reilinger R, Romeyeh MA, Alsouod A, Yassminh R, Ballani B, Darawcheh R, Sbeinati R, Radwan Y, Masri RA, Bayerly M, Ghazzi RA, Barazangi M (2010) Crustal deformation in northwestern Arabia from GPS measurements in Syria: slow slip rate along the northern Dead Sea Fault. Geophys J Int 180:125–135

Altunel E, Meghraoui M, Karabacak V, Akyuz SH, Ferry M, Yalciner CC, Munschy M (2009) Archaeological sites (Tell and Road) offset by the Dead Sea Fault in the Amik Basin, Southern Turkey. Geophys J Int 179:1313–1329

Ambraseys NN (2005) The seismic activity in Syria and Palestine during the Middle of the 8th century; an amalgamation of historical earthquakes. J Seismol 9:115–125

Ambraseys NN (2009) Earthquakes in the Mediterranean and Middle East: a multidisciplinary study of seismicity up to 1900. Cambridge University Press, Cambridge, UK

Ambraseys NN, Barazangi M (1989) The 1759 earthquake in the Bekaa valley: implications for earthquake hazard assessment in the eastern Mediterranean region. J Geophys Res 94:4007–4013

Ambraseys NN, Finkel CF (1995) The seismicity of Turkey and adjacent areas, a historical review, 1500–1800. Eren, Istanbul

Ambraseys NN, Melville CP (1988) An analysis of the eastern Mediterranean earthquake of 20 May 1202. In: Lee WKH, Meyers H, Shimazaki K (eds) Historical seismograms and earthquakes of the world. Academic, San Diego, pp 181–200

Ambraseys NN, Melville CP, Adams RD (1994) The seismicity of Egypt, Arabia, and the Red Sea: a historical review. Cambridge University Press, Cambridge, UK

Amiran DHK, Arieh E, Turcotte T (1994) Earthquakes in Israel and adjacent areas: Macroseismic observations since 100 B.C.E. Isr Explor J 44:260–305

Amit R, Harrison JBJ, Enzel Y (1995) Use of soils and colluvial deposits in analyzing tectonic events – The Southern Arava Rift, Israel. Geomorphology 12:91–107

Amit R, Harrison JBJ, Enzel Y, Porat N (1996) Soils as a tool for estimating ages of Quaternary fault scarps in a hyperarid environment – The southern Arava Valley, the Dead Sea rift, Israel. Catena 28:21–45

Amit R, Zilberman E, Porat N, Enzel Y (1999) Relief inversion in the Avrona Playa as evidence of large-magnitude historical earthquakes, southern Arava Valley, Dead Sea rift. Quat Res 52:76–91

Amit R, Zilberman E, Enzel Y, Porat N (2002) Paleoseismic evidence for time dependency of seismic response on a fault system in the southern Arava valley, Dead Sea rift. Isr Geol Soc Am Bull 114:192–206

Baer G, Sandwell D, Williams S, Bock Y, Shamir G (1999) Coseismic deformation associated with the November 1995, Mw = 7.1 Nuweiba earthquake, Gulf of Elat (Aqaba), detected by synthetic aperture radar interferometry. J Geophys Res 104:25221–225232

Bakun WH, Wentworth CM (1998) Estimating earthquake location and magnitude from seismic intensity data. Bull Seismol Soc Am 87:1502–1521

Barka A (1996) Slip distribution along the North Anatolian Fault associated with the large earthquakes of the period 1939 to 1967. Bull Seismol Soc Am 86:1238–1254

Bartov Y, Sagy A (2004) Late Pleistocene extension and strike-slip in the Dead Sea Basin. Geol Mag 141:565–572

Bartov Y, Steinitz G, Eyal M, Eyal Y (1980) Sinistral movement along the Gulf of Aqaba – Its age and relation to the opening of the Red Sea. Nature 285:220–221

Bartov Y, Sneh A, Fleischer L, Arad V, Rosensaft M (2002) Map of suspect active faults in Israel. The Geological Survey of Israel, Jerusalem

Basson U, Ben-Avraham Z, Garfunkel Z, Lyakhovsky V (2002) Development of recent faulting in the southern Dead Sea rift according to GPR imaging. EGS Stephan Mueller Spec Publ Ser 2:1–23

Ben-Avraham Z, Garfunkel Z (1979) Continental breakup by a leaky transform: the Gulf of Elat (Aqaba). Science 206:214–216

Ben-Menahem A (1981) Variation of slip and creep along the Levant Rift over the past 4500 years. Tectonophysics 80:183–197
Butler RWH, Spencer S, Griffiths HM (1997) Transcurrent fault activity on the Dead Sea Transform in Lebanon and its implications for plate tectonics and seismic hazard. J Geol Soc 154:757–760
Butler RWH, Spencer S, Griffiths HM (1999) Discussion on transcurrent fault activity on the Dead Sea Transform in Lebanon and its implications for plate tectonics and seismic hazard – Reply. J Geol Soc 156:1246–1248
Chaimov TA, Barazangi M (1990) Crustal shortening in the Palmyride fold belt, Syria, and implications for movement along the Dead Sea Fault system. Tectonics 9:1369–1386
Chorowicz J, Dhont D, Ammar O, Rukieh M, Bilal A (2005) Tectonics of the Pliocene Homs basalts (Syria) and implications for the Dead Sea Fault Zone activity. J Geol Soc 162:259–271
Daëron M, Benedetti L, Tapponnier P, Sursock A, Finkel RC (2004) Constraints on the post 25-ka slip rate of the Yammouneh fault (Lebanon) using in situ cosmogenic 36Cl dating of offset limestone-clast fans. Earth Planet Sci Lett 227:105–119
Daëron M, Klinger Y, Tapponnier P, Elias A, Jacques E, Sursock A (2005) Sources of the large AD 1202 and 1759 Near East earthquakes. Geology 33:529–532
Daëron M, Klinger Y, Tapponnier P, Elias A, Jacques E, Sursock A (2007) 12,000-year-long record of 10 to 13 paleoearthquakes on the Yammouneh Fault, Levant Fault system, Lebanon. Bull Seismol Soc Am 97:749–771
Dubertret L (1932) Les formes structurales de la Syrie et de la Palestine. Académie des Sciences Comptes Rendus 195:65–67
Dubertret L (1947) Problemes de la geologic du Levant. Bull Soc Geol Fr Ser 5:3–31
Elias A, Tapponnier P, Singh SC, King GCP, Briais A, Daëron M, Carton H, Sursock A, Jacques E, Jomaa R, Klinger Y (2007) Active thrusting offshore Mount Lebanon: source of the tsunamigenic A.D. 551 Beirut-Tripoli earthquake. Geology 35:755–758
El-Isa ZH, Mustafa H (1986) Earthquake deformations in the Lisan deposits and seismotectonic implications. Geophys J R Astron Soc 86:413–424
Ellenblum R, Marco S, Agnon A, Rockwell T, Boas A (1998) Crusader castle torn apart by earthquake at dawn, 20 May 1202. Geology 26:303–306
Enzel Y, Kadan G, Eyal Y (2000) Holocene earthquakes inferred from a fan-delta sequence in the Dead Sea graben. Quat Res 53:34–48
Eyal Y, Reches Z (1983) Tectonic analysis of the Dead Sea rift region since the Late-Cretaceous based on mesostructures. Tectonics 2:39–66
Eyal M, Eyal Y, Bartov Y, Steinitz G (1981) The tectonic development of the western margin of the Gulf of Elat (Aqaba) rift. Tectonophysics 80:39–66
Ferry M, Meghraoui M (2008) Reply to the comment of Dr M. Klein on: "A 48-kyr-long slip rate history for the Jordan Valley segment of the Dead Sea Fault". Earth Planet Sci Lett 268:241–242
Ferry M, Meghraoui M, Abou Karaki N, Al-Taj M, Amoush H, Al-Dhaisat S, Barjous M (2007) A 48-kyr-long slip rate history for the Jordan Valley segment of the Dead Sea Fault. Earth Planet Sci Lett 260:394–406
Ferry M, Meghraoui M, Abou Karaki N, Al-Taj M, Khalil L (2011) Episodic behavior of the Jordan Valley section of the Dead Sea fault inferred from a 14-ka-long integrated catalog of large earthquakes. Bull Seismol Soc Am 101:39–67
Fleury J, Chorowicz J, Somma J (1999) Discussion on transcurrent fault activity on the Dead Sea Transform in Lebanon and its implications for plate tectonics and seismic hazard. J Geol Soc 156:1243–1248
Freund R (1965) A model of the structural development of Israel and adjacent areas since Upper Cretaceous times. Geol Mag 102:189–205
Freund R, Zak I, Garfunkel Z (1968) Age and rate of the sinistral movement along the Dead Sea Rift. Nature 220:253–255
Freund R, Garfunkel Z, Zak I, Goldberg M, Weissbrod T, Derin B (1970) The shear along the Dead Sea rift. Philos Trans R Soc Lond A 267:107–130
Frieslander U (2000) The structure of the Dead Sea Transform emphasizing the Arava using new geophysical data. The Hebrew University of Jerusalem, p 101

Galli P (1999) Active tectonics along the Wadi Araba-Jordan Valley transform fault. J Geophys Res 104:2777–2796
Gardosh M, Reches Z, Garfunkel Z (1990) Holocene tectonic deformation along the western margins of the Dead Sea. Tectonophysics 180:123–137
Garfunkel Z (1981) Internal structure of the Dead Sea leaky transform (rift) in relation to plate kinematics. Tectonophysics 80:81–108
Garfunkel Z (2011) The long- and short-term lateral slip and seismicity along the Dead Sea Transform: an interim evaluation. Isr J Earth Sci 58:217–235
Garfunkel Z, Zak I, Freund R (1981) Active faulting in the Dead Sea rift. Tectonophysics 80:1–26
Gerson R, Grossman S, Amit R, Greenbaum N (1993) Indicators of faulting events and periods of quiescence in desert alluvial fans. Earth Surf Proc Land 18:181–202
Ginat H, Enzel Y, Avni Y (1998) Translocation of Plio-Pleistocene drainage system along the Dead Sea Transform, south Israel. Tectonophysics 284:151–160
Girdler RW (1990) The Dead-Sea Transform-Fault system. Tectonophysics 180:1–13
Gomez F, Meghraoui M, Darkal AN, Sbeinati R, Darawcheh R, Tabet C, Khawlie M, Charabe M, Khair K, Barazangi M (2001) Coseismic displacements along the Serghaya fault: an active branch of the Dead Sea Fault system in Syria and Lebanon. J Geol Soc 158:405–408
Gomez F, Meghraoui M, Darkal AN, Hijazi F, Mouty M, Suleiman Y, Sbeinati R, Darawcheh R, Al-Ghazzi R, Barazangi M (2003) Holocene faulting and earthquake recurrence along the Serghaya branch of the Dead Sea fault system in Syria and Lebanon. Geophys J Int 153:658–674
Gomez F, Karam G, Khawlie M, McClusky S, Vernant P, Reilinger R, Jaafar R, Tabet C, Khair K, Barazangi M (2007) Global Positioning System measurements of strain accumulation and slip transfer through the restraining bend along the Dead Sea fault system in Lebanon. Geophys J Int 168:1021–1028
Guidoboni E, Comastri A (2005) Catalogue of earthquakes and tsunamis in the Mediterranean area from the 11th to the 15th century. Istituto Nazionale di Geofisica, Bologna
Guidoboni E, Comastri A, Traina G (1994) Catalogue of ancient earthquakes in the Mediterranean area up to the 10th century. Istituto Nazionale di Geofisica, Bologna
Haynes JM, Niemi TM, Atallah M (2006) Evidence for ground-rupturing earthquakes on the Northern Wadi Araba fault at the archaeological site of Qasr Tilah, Dead Sea Transform fault system, Jordan. J Seismol 10:415–430
Hazan N, Stein M, Marco S (2004) Lake Kinneret levels and active faulting in the Tiberias area. Isr J Earth Sci 53:199–205
Heimann A (1990) The development of the Dead Sea rift and its margins in the northern Israel during the Pliocene and the Pleistocene. Golan Research Institute and Geological Survey of Israel, Jerusalem
Heimann A, Ron H (1987) Young faults in the Hula pull-apart basin, central Dead Sea Transform. Tectonophysics 141:117–124
Heimann A, Ron H (1993) Geometric changes of plate boundaries along part of the northern Dead Sea Transform: geochronologic and paleomagnetic evidence. Tectonics 12:477–491
Hofstetter R, Klinger Y, Amrat AQ, Rivera L, Dorbath L (2007) Stress tensor and focal mechanisms along the Dead Sea fault and related structural elements based on seismological data. Tectonophysics 429(3–4):165–181
Joffe S, Garfunkel Z (1987) Plate kinematics of the circum Red Sea- a re-evaluation. Tectonophysics 141:5–22
Karabacak V, Altunel E, Meghraoui M, Akyüz H (2010) Field evidences from northern Dead Sea Fault Zone (South Turkey): new findings for the initiation age and slip rate. Tectonophysics 480:172–182
Klein M (2008) A comment on: "A 48-kyr-long slip rate history for the Jordan Valley segment of the Dead Sea Fault" EPSL 260 (2007) 394–406. Earth Planet Sci Lett 268:239–240
Klinger Y, Rivera L, Haessler H, Maurin JC (1999) Active faulting in the Gulf of Aqaba: new knowledge from the Mw7.3 earthquake of 22 November 1995. Bull Seismol Soc Am 89:1025–1036
Klinger Y, Avouac JP, Abou-Karaki N, Dorbath L, Bourles D, Reyss JL (2000a) Slip rate on the Dead Sea Transform fault in northern Araba Valley (Jordan). Geophys J Int 142:755–768

Klinger Y, Avouac JP, Dorbath L, Abou-Karaki N, Tisnerat N (2000b) Seismic behaviour of the Dead Sea Fault along Araba Valley. Jordan Geophys J Int 142:769–782
Le Beon M, Klinger Y, Amrat AQ, Agnon A, Dorbath L, Baer G, Ruegg JC, CharadeO, Mayyas O (2008) Slip rate and locking depth from GPS profiles across the southern Dead Sea Transform. J Geophys Res Solid Earth 113:B11403, pp 19
Le Beon M, Klinger Y, Al-Qaryouti M, Meriaux AS, Finkel RC, Elias A, Mayyas O, Ryerson FJ, Tapponnier P (2010) Early Holocene and Late Pleistocene slip rates of the southern Dead Sea Fault determined from Be-10 cosmogenic dating of offset alluvial deposits. J Geophys Res Solid Earth 115:B11414, pp 24
Le Beon M, Klinger Y, Meriaux AS, Al-Qaryouti M, Finkel RC, Mayyas O, Tapponnier P (2012) Quaternary morphotectonic mapping of the Wadi Araba and implications for the tectonic activity of the southern Dead Sea fault. Tectonics 31:TC5003, pp 25
Mahmoud S, Reilinger R, McClusky S, Vernant P, Tealeb A (2005) GPS evidence for northward motion of the Sinai Block: implications for E. Mediterranean tectonics. Earth Planet Sci Lett 238:217–224
Makovsky Y, Wunch A, Ariely R, Shaked Y, Rivlin A, Shemesh A, Ben Avraham Z, Agnon A (2008) Quaternary transform kinematics constrained by sequence stratigraphy and submerged coastline features: the Gulf of Aqaba. Earth Planet Sci Lett 271:109–122
Marco S (2007) Temporal variation in the geometry of a strike-slip fault zone: examples from the Dead Sea Transform. Tectonophysics 445:186–199
Marco S (2008) Recognition of earthquake-related damage in archaeological sites: examples from the Dead Sea fault zone. Tectonophysics 453:148–156
Marco S, Agnon A (1995) Prehistoric earthquake deformations near Masada, Dead Sea graben. Geology 23:695–698
Marco S, Agnon A (2005) High-resolution stratigraphy reveals repeated earthquake faulting in the Masada Fault Zone, Dead Sea Transform. Tectonophysics 408:101–112
Marco S, Agnon A, Ellenblum R, Eidelman A, Basson U, Boas A (1997) 817-year-old walls offset sinistrally 2.1 m by the Dead Sea Transform, Israel. J Geodyn 24:11–20
Marco S, Hartal M, Hazan N, Lev L, Stein M (2003) Archaeology, history, and geology of the A.D. 749 earthquake, Dead Sea Transform. Geology 31:665–668. doi:10.1130/G19516.19511
Marco S, Rockwell TK, Heimann A, Frieslander U, Agnon A (2005) Late Holocene slip of the Dead Sea Transform revealed in 3D palaeoseismic trenches on the Jordan Gorge segment. Earth Planet Sci Lett 234:189–205
Marco S, Stein M, Agnon A, Ron H (1996) Long-term earthquake clustering: a 50,000-year paleoseismic record in the Dead Sea Graben. J Geophys Res-Solid Earth 101(B3):6179–6191
McClusky S, Reilinger R, Mahmoud S, Sari DB, Tealeb A (2003) GPS constraints on Africa (Nubia) and Arabia plate motions. Geophys J Int 155:126
Meghraoui M, Gomez F, Sbeinati R, derWoerd JV, Mouty M, Darkal AN, Radwan Y, Layyous I, Najjar HA, Darawcheh R, Hijazi F, Al-Ghazzi R, Barazangi M (2003) Evidence for 830 years of seismic quiescence from palaeoseismology, archaeoseismology and historical seismicity along the Dead Sea fault in Syria. Earth Planet Sci Lett 210:35–52
Nemer T, Meghraoui M (2006) Evidence of coseismic ruptures along the Roum fault (Lebanon): a possible source for the AD 1837 earthquake. J Struct Geol 28:1483–1495
Nemer T, Meghraoui M, Khair K (2008) The Rachaya-Serghaya fault system (Lebanon): evidence of coseismic ruptures, and the AD 1759 earthquake sequence. J Geophys Res 113:B05312
Niemi TM, Zhang H, Atallah M, Harrison BJ (2001) Late Pleistocene and Holocene slip rate of the Northern Wadi Araba fault, Dead Sea Transform, Jordan. J Seismol 5:449–474
Pe'eri S, Wdowinski S, Shtibelman A, Bechor N (2002) Current plate motion across the Dead Sea Fault from three years of continuous GPS monitoring. Geophys Res Lett 29:42–45. doi:10.1029/2001GL013879
Pinar A, Turkelli N (1997) Source inversion of the 1993 and 1995 Gulf of Aqaba earthquakes. Tectonophysics 283:279–288
Quennell AM (1956) Tectonics of the Dead Sea rift. In: Asociacion de Servicios Geologicos Africanos. Congreso Geologico Internacional, 20th sesion, Mexico, pp 385–405

Reches Z, Hoexter DF (1981) Holocene seismic and tectonic activity in the Dead Sea area. Tectonophysics 80:235–254

Reilinger R, McClusky S, Vernant P, Lawrence S, Ergintav S, Cakmak R, Ozener H, Kadirov F, Guliev I, Stepanyan R, Nadariya M, Hahubia G, Mahmoud S, Sakr K, ArRajehi A, Paradissis D, Al-Aydrus A, Prilepin M, Guseva T, Evren E, Dmitrotsa A, Filikov SV, Gomez F, Al-Ghazzi R, Karam G (2006) GPS constraints on continental deformation in the Africa-Arabia-Eurasia continental collision zone and implications for the dynamics of plate interactions. J Geophys Res Solid Earth 111:B05411, pp 26

Ron H, Freund R, Garfunkel Z, Nur A (1984) Block-rotation by strike-slip faulting: structural and paleomagnetic evidence. J Geophys Res 89:6256–6270

Rotstein Y, Bartov Y, Frieslander U (1992) Evidence for local shifting of the main fault and changes in the structural setting, Kinarot basin, Dead Sea Transform. Geology 20:251–254

Rucker JD, Niemi TM (2010) Historical earthquake catalogues and archaeological data: achieving synthesis without circular reasoning. In: Sintubin M, Stewart IS, Niemi TM, Altunel E (eds) Ancient earthquakes, The Geological Society of America special paper. The Geological Society of America, Boulder, pp 97–106

Russell KE (1985) The earthquake chronology of Palestine and northwest Arabia from the 2nd through the mid-8th century A.D. Bull Am Sch Orient Res 260:37–60

Sadeh M, Hamiel Y, Ziv A, Bock Y, Fang P, Wdowinski S (2012) Crustal deformation along the Dead Sea Transform and the Carmel Fault inferred from 12 years of GPS measurements. J Geophys Res Solid Earth 117:B08410

Salamon A, Hofstetter A, Garfunkel Z, Ron H (1996) Seismicity of the eastern Mediterranean region: perspective from the Sinai subplate. Tectonophysics 263:293–305

Sbeinati MR, Darawcheh R, Mouty M (2005) The historical earthquakes of Syria: an analysis of large and moderate earthquakes from 1365 B.C. to 1900 A.D. Ann Geophys 48:347–435

Shaked Y, Lazar B, Marco S, Stein M, Tchernov D, Agnon A (2004) Detailed evolution of fringing reefs: space and time constraints from the Gulf of Aqaba. Coral Reefs 24:165–172. DOI:10.1007/s00338-004-0454-2

Shaked Y, Lazar B, Marco S, Stein M, Agnon A (2012) Late holocene events that shaped the shoreline at the northern Gulf of Aqaba recorded by a buried fossil reef. Israel J Earth Sci 58(3–4):355–368

Shaliv G (1991) Stages in the tectonic and volcanic history of the Neogene basin in the Lower Galilee and the valleys. Geological Survey of Israel – Report (in Hebrew, English abstract) 11/91, pp 1–94

Shamir G, Baer G, Hofstetter A (2003) Three-dimensional elastic earthquake modelling based on integrated seismological and InSAR data: the Mw = 7.2 Nuweiba earthquake, gulf of Elat/Aqaba 1995 November. Geophys J Int 154:731–744

Sieberg A (1932) Erdbebengeographie, Handbuch der Geophysik, Band IV. Borntraeger, Berlin, pp 527–1005

Sirovich L, Pettenati F, Cavallini F, Bobbio M (2002) Natural-neighbor isoseismals. Bull Seismol Soc Am 92:1933–1940

Stein RS, Barka A, Dietrich JH (1997) Progressive failure on the North Anatolian fault since 1939 by earthquake stress triggering. Geophys J Int 128:594–604

Steinitz G, Bartov Y (1986) The 1985 time table for the tectonic events along the Dead Sea Transform. Terra Cognita 6:160

ten Brink US, Rybakov M, Al-Zoubi AS, Hassouneh M, Frieslander U, Batayneh AT, Goldschmidt V, Daoud MN, Rotstein Y, Hall JK (1999) Anatomy of the Dead Sea Transform: does it reflect continuous changes in plate motion? Geology 27:887–890

ten-Brink US, Ben-Avraham Z (1989) The anatomy of a pull-apart basin: reflection observations of the Dead Sea Basin. Tectonics 8:333–350

Thomas R, Niemi TM, Parker ST (2007) Structural damage from earthquakes in the second-ninth centuries at the archaeological site of Aila in Aqaba, Jordan. Bull Am Sch Orient Res 346:59–77

Vroman AJ (1973) Is a compromise between the theories of tension and of shear for the origin of the Jordan-Dead Sea trench possible? Isr J Earth Sci 22:141–156

Wdowinski S, Bock Y, Baer G, Prawirodirdjo L, Bechor N, Naaman S, Knafo R, Forrai Y, Melzer Y (2004) GPS Measurements of current crustal movements along the Dead Sea Fault. J Geophys Res 109:1–16

Wechsler N, Rockwell TK, Klinger Y, Agnon A, Marco S (2011) Testing earthquake recurrence models with 3D trenching along the Dead-Sea Transform, 2nd INQUA-IGCP-567 International Workshop on Active Tectonics, Earthquake Geology, Archaeology and Engineering, Corinth, Greece

Wells DL, Coppersmith KJ (1994) New empirical relationships among magnitudes, rupture length, rupture width, rupture area, and surface displacement. Bull Seismol Soc Am 84:974–1002

Willis B (1938) Wellings' observations of Dead Sea structure (with discussion). Geol Soc Am Bull 49:659–668

Wilson JT (1965) A new class of faults and their bearing on continental drift. Nature 207:343–347

Zilberman E, Amit R, Heimann A, Porat N (2000) Changes in Holocene paleoseismic activity in the Hula pull-apart basin, Dead Sea rift, northern Israel. Tectonophysics 321:237–252

Zilberman E, Amit R, Porat N, Enzel Y, Avner U (2005) Surface ruptures induced by the devastating 1068 AD earthquake in the southern Arava valley, Dead Sea rift, Israel. Tectonophysics 408:79–99

Zohar M, Marco S (2012) Re-estimating the epicenter of the 1927 Jericho earthquake using spatial distribution of intensity data. J Appl Geophys 82:19–29